

ISENTROPIC OBJECTIVE ANALYSIS
OF
CLEAR-AIR TURBULENCE PARAMETERS

by

MARK P. LUTZ

B.S., University of Washington
1971

SUBMITTED IN PARTIAL FULFILLMENT OF THE
REQUIREMENTS FOR THE DEGREE OF MASTER OF SCIENCE
at the
MASSACHUSETTS INSTITUTE OF TECHNOLOGY
June 1973

Signature of Author Department of Meteorology, 16 May 1973

Certified by Thesis Supervisor

Accepted by Chairman, Departmental Committee on Graduate Students

Lindgren
WITHDRAWN
MASS. INST. TECH.
MAY 31 1973
MIT LIBRARIES

ISENTROPIC OBJECTIVE ANALYSIS
OF
CLEAR-AIR TURBULENCE PARAMETERS
by
MARK P. LUTZ

Submitted to the Department of Meteorology on 16
May 1973 in partial fulfillment of the require-
ments for the degree of Master of Science

ABSTRACT

Computers are used to prepare fine-scale isobaric analyses interpolated from objective isentropic analyses made from radiosonde observations. Geostrophic Richardson numbers are calculated from the analyses and compared with aircraft reports of clear-air turbulence. The aircraft reports are divided into categories on the basis of jet-stream speed, cyclonic or anticyclonic streamline curvature, and whether or not the terrain below was mountainous. The relationship of these groups to the Richardson numbers is also studied.

The results show a significant association between the occurrences of clear-air turbulence and the computed Richardson numbers. The association is found to be stronger for anticyclonic instances than for cyclonic ones, for non-mountain instances than for mountainous ones, and for cases where the maximum jet-stream speed is less than 60 m sec^{-1} than for cases where it is greater than 60 m sec^{-1} .

Thesis Supervisor: Frederick Sanders
Title: Professor of Meteorology

ACKNOWLEDGEMENT

Of the many people who helped with this study, the author would particularly like to thank his advisor, Professor Frederick Sanders, for his constant guidance and encouragement; Dr. Melvyn Shapiro of the National Center for Atmospheric Research for suggesting the idea and for helping with the computer analysis; Dr. Rainer Bleck of NCAR for providing the objective analysis programs and for many helpful suggestions; Professor James A. Woods of Penn. State for supplying the aircraft reports; Nelson Seaman of Penn. State for providing the balanced stream function program; and Miss Isabel Kole for help with preparing the figures.

The National Center for Atmospheric Research, which is sponsored by the Nation Science Foundation, is also thanked for making available the computer time used in this research.

Part of the support for this project came from the National Science Foundation, Atmospheric Sciences Section, under grant GA-28203X.

TABLE OF CONTENTS

ABSTRACT	2
ACKNOWLEDGEMENT	3
TABLE OF CONTENTS	4
LIST OF SYMBOLS	5
I. INTRODUCTION	7
A. Clear-air turbulence	7
B. Isentropic analysis	8
C. Objectives	10
II. PROCEDURE	11
III. RESULTS	19
IV. CONCLUSIONS	22
TABLE 1	25
FIGURES	26-47
REFERENCES	48

LIST OF SYMBOLS

C_p	specific heat of dry air at constant pressure
f	Coriolis parameter
g	acceleration of gravity
p	pressure
p_0	reference pressure, 1000 mb
R	gas constant for dry air
T	absolute temperature
\vec{u}	horizontal wind
\vec{u}_{bal}	balanced wind
\vec{u}_g	geostrophic wind
x, y, z	cartesian coordinates
α	specific volume
θ	potential temperature
κ	R/C_p
ρ	density
Ψ_m	Montgomery potential

∇ horizontal gradient operator

$()_p$ evaluated at constant p

I. INTRODUCTION

A. Clear-air Turbulence

Clear-air turbulence is a small-scale atmospheric phenomenon which occurs when an unstable Kelvin-Helmholtz wave breaks, converting potential into kinetic energy. The presence of Kelvin-Helmholtz instability depends principally on two things: the static stability and the vertical wind shear of the atmosphere. For this reason, the Richardson number, which combines these two factors, is most commonly used as an indicator of the likelihood of clear-air turbulence:

$$Ri = \frac{g}{\theta} \frac{\partial \theta / \partial z}{|\partial \vec{v} / \partial z|^2}$$

Although first proposed in 1920 in connection with energetics of atmospheric eddies, it is now used almost exclusively with reference to CAT. Theoretical studies have shown that Ri needs to be less than .25 for the Kelvin-Helmholtz wave to break (Taylor, 1931). The many empirical studies of clear-air turbulence which have been carried out in recent years have tended to confirm this threshold value (Panofsky et al., 1968; Reed, 1969).

The use of radiosonde observations to study CAT is not considered feasible since data is needed at exactly the time and place of its occurrence. The most usual ways, therefore, of examining clear-air turbulence are with reconnaissance aircraft and radar, or a combination of both. The radar is used mainly to determine the location and extent of the CAT, by means of the resulting differ-

ences in refractive index. The aircraft, on the other hand, are used to carry aloft instruments to measure the vertical profiles of temperature and wind. Using this approach, Reed and Hardy (1972) investigated a widespread outbreak of CAT in an upper level frontal zone. They identified three types of CAT with wavelengths ranging from 1.6 to 30 km. They showed that anticyclonic curvature was important in producing supergeostrophic winds and wind shears, thus helping to make R_i small. It was also noted that a large shear is relatively more important than a small stability in producing a small R_i . Browning (1971) found that the layers of low stability and of large wind shear in which CAT occurs have depths on the order of 200m and 600m, respectively. Waco (1972) reported that planes encountering clear-air turbulence flew through horizontal temperature changes of 10°C or more in 5 miles, indicative of strong vertical shear.

B. Isentropic Analysis

Isentropic analysis has long been regarded as superior for certain uses to the more conventional isobaric analysis for two reasons: 1) isentropic surfaces are a much closer approximation to "material" surfaces than are isobaric surfaces; that is, individual parcels of air tend to move more nearly along isentropic than along isobaric surfaces, and 2) much of the fine-scale vertical structure in radiosonde data can be retained in an isentropic analysis, but is lost when merely interpolating between stations on isobaric surfaces. This is due to the fact that the distribution of meteorological parameters tends to be smoother

on isentropic surfaces than on isobaric ones.

The feasibility of isentropic analysis was improved by R.B. Montgomery, who, in 1937, introduced the so-called "Montgomery potential,"

$$\Psi_m = C_p T + gz,$$

the isentropic gradient of which represents the horizontal pressure-gradient force per unit mass. Thus, isolines of Ψ_m serve to determine the flow on isentropic surfaces the way height contours do for constant pressure surfaces, and isobars for constant height surfaces.

Following an early period of enthusiastic application, however, isentropic analysis fell into disuse since it was felt that T would have to be measured within $\pm 0.1^\circ\text{C}$ to achieve sufficient accuracy in the geostrophic wind. It was not until 1959, when Danielsen destroyed this myth, that isentropic analysis regained some measure of favor. He showed that since, for a given value of θ , a p is determined to find z hydrostatically, this p can also be used to establish T through Poisson's equation. Ψ_m can therefore be computed as accurately as z can be measured, which is sufficient for most uses. Isentropic analysis is still not widely used, but a recent study by Bosart (1969) illustrated its usefulness in regard to mid-tropospheric frontogenesis, many of the characteristics of which are also important in clear-air turbulence.

C. Objectives

Even though synoptic-scale data is not generally used to study clear-air turbulence, it was felt that fine-scale isentropic analyses might be enough better than the usual isobaric analyses to produce useful results. This investigation attempts to establish Richardson numbers computed from such analyses as a predictor of regions where CAT may be expected to occur. The analysis procedure for computing the Richardson numbers is admittedly somewhat crude, but should isentropic prediction models come into use some time in the near future, computer time restrictions may limit the use of anything more sophisticated. Thus, perhaps the method used here is a realistic one.

II. PROCEDURE

The procedure, in a nutshell, consists of preparing isentropic analyses, with the aid of the NCAR computers, for various synoptic times, computing Richardson numbers from the analyses, and correlating these Richardson numbers with aircraft observations of clear air-turbulence.

A collection of some 68,000 reports made by American Airlines pilots during 1969 and 1970 was obtained. These reports include the plane's location, to the nearest degree of latitude and longitude, its elevation in thousands of feet, the intensity of turbulence being encountered, if any, and the time the observation was made, to the nearest hour. The reports which fell near radiosonde observation times (0700 and 1900EST) were inspected, and 16 such times were chosen for study because of the large number of reports with at least light turbulence which they exhibited. Because of the greater number of planes in the air at 1900EST compared to 0700EST, there were many more reports at or near this time, and, hence, only one 0700EST case was chosen.

Isentropic objective analyses were prepared for these times, based on a scheme developed by the author and others at NCAR. The analyzed area is a 21x21 subset of the NMC northern hemisphere grid which covers most of North America (Fig. 1).

The first and second steps were developed by Rainer Bleck (Bleck and Haagenson, 1968) for use with his isentropic forecasting models. The first step computes values of Ψ_m on isentropic

surfaces at the stations in the grid from their respective radiosonde observations. This is a relatively simple matter, since the coded radiosonde data has T and z at several levels. However, it is done rather carefully by recalculating all the heights from the temperature and pressure profiles in case there are errors in the transmitted data. We had hoped to make calculations for isentropic levels at $2\frac{1}{2}^{\circ}$ intervals, but small-scale features in the individual soundings led to computational problems which have so far proved intractable.* A 5° interval was therefore used, with θ ranging from 260°K to 380°K .

The second step, which is really the heart of the procedure, is an objective analysis of Ψ_m on the θ -surfaces. Grid-point values are computed from the station values, using an Eddy regression method (Eddy, 1967). A "first-guess" field is made, and then improved upon by applying Eddy's method to the differences between the radiosonde values and the first-guess values at the stations. The grid-point differences so-computed are added to the grid-point values of the first-guess field. The process is repeated until sufficient accuracy is achieved. The differences between the actual winds and the geostrophic winds are analyzed in similar fashion and used to improve the first-guess field as a further refinement.

At this point, the first and second derivatives of Ψ_m with respect to θ are also computed, with a finite difference scheme.

* Personal communication with Dave Fulker of the NCAR Computing Facility staff.

The first derivative yields a function of the pressure:

$$\begin{aligned}\Psi_m &= c_p T + gz \\ &= c_p \theta \left(\frac{p}{p_0}\right)^k + gz\end{aligned}$$

$$\frac{d\Psi_m}{d\theta} = c_p \left(\frac{p}{p_0}\right)^k .$$

These numbers are used in the interpolation onto isobaric surfaces. A more straight-forward method of analyzing pressure on isentropic surfaces without finite differencing might lead to better results.

The second derivative yields a function of the static stability:

$$\begin{aligned}\frac{d^2\Psi_m}{d\theta^2} &= c_p \frac{d}{d\theta} \left[\left(\frac{p}{p_0}\right)^k \right] \\ &= \frac{c_p k}{p_0} \left(\frac{p}{p_0}\right)^{k-1} \frac{dp}{d\theta} \\ \frac{dp}{d\theta} &= \frac{p_0}{c_p k} \left(\frac{p}{p_0}\right)^{1-k} \frac{d^2\Psi_m}{d\theta^2}\end{aligned}$$

This $dp/d\theta$ is used in the calculation of the Richardson number.

The third step, developed by Nelson Seaman of Penn. State (1972), solves a form of the balance equation to obtain a balanced stream function from Ψ_m . A simple finite-difference scheme yields the balanced wind field on isentropic surfaces. It was decided that small-scale variability in the actual reported wind field made an objective analysis of it impractical. Hence, the

use of a theoretical wind field. Furthermore, it was felt that, due to the curvature of the streamlines present in most cases, a balanced wind would be more accurate than the geostrophic wind.

A short step at this point was used to compute the magnitude of the horizontal gradient of potential temperature, a part of the geostrophic vertical wind shear. Since this will later be analyzed on isobaric surfaces, $|\nabla\theta|$ at constant p is needed:

$$|\nabla\theta|_p = \sqrt{\left(\frac{\partial\theta}{\partial x}\right)_p^2 + \left(\frac{\partial\theta}{\partial y}\right)_p^2}$$

$$\left(\frac{\partial\theta}{\partial x}\right)_p = \left(\frac{\partial\theta}{\partial x}\right)_\theta - \left(\frac{\partial p}{\partial x}\right)_\theta \left(\frac{d\theta}{dp}\right)$$

$$= -\left(\frac{\partial p}{\partial x}\right)_\theta \left(\frac{d\theta}{dp}\right)$$

$$\left(\frac{\partial\theta}{\partial y}\right)_p = \left(\frac{\partial\theta}{\partial y}\right)_\theta - \left(\frac{\partial p}{\partial y}\right)_\theta \left(\frac{d\theta}{dp}\right)$$

$$= -\left(\frac{\partial p}{\partial y}\right)_\theta \left(\frac{d\theta}{dp}\right)$$

$$|\nabla\theta|_p = \sqrt{\left(\frac{\partial p}{\partial x}\right)_\theta^2 \left(\frac{d\theta}{dp}\right)^2 + \left(\frac{\partial p}{\partial y}\right)_\theta^2 \left(\frac{d\theta}{dp}\right)^2}$$

$$= \frac{d\theta}{dp} \sqrt{\left(\frac{\partial p}{\partial x}\right)_\theta^2 + \left(\frac{\partial p}{\partial y}\right)_\theta^2}$$

The $\partial p/\partial x$'s and $\partial p/\partial y$'s were obtained through simple centered finite differencing (uncentered at the boundaries); $d\theta/dp$ is merely the reciprocal of the previously computed $dp/d\theta$.

An attempt was made to compute $\partial\vec{u}/\partial p$ (through vertical finite differencing of the balanced wind) and from it a Richardson num-

ber. However, discrepancies between the observed winds and the balanced wind fields made these results unsatisfactory. Hence, the balanced winds were used only as an indicator of the maximum jet-stream speed, and only a geostrophic Richardson number was used.

The final analysis step was developed by the author while at NCAR (Lutz, 1972) and subsequently modified. In its present form, it computes fields of z , p , and $dp/d\theta$ and interpolates the results, along with fields of $|\vec{u}_{bal}|$, $|\nabla\theta|$, and θ itself, onto four constant pressure surfaces: 350, 300, 250, and 200 mb. These levels were chosen since nearly all of the aircraft reports were in this region of the atmosphere. A horizontal interpolation, by means of bicubic splines, is done first to reduce the grid interval. The bicubic spline (Nilson, 1970) is a form of cubic fit which not only insures a perfect fit at each grid point, but which also makes the first and second derivatives continuous.

Since most of the aircraft reports were in the eastern United States, only one quarter of the original grid (an 11x11 subset) was used. This allowed the NMC grid to be reduced by a factor of 6, to approximately 60 km. A second interpolation is done in the vertical, also using splines (Walsh et al., 1962), which computes the values on isobaric surfaces. In the case of $|\nabla\theta|$, the large vertical and horizontal variations necessitated the use of a spline under tension (Schweikert, 1966). This is essentially a "tightening" of the fit to somewhere between linear and pure spline. The spline was "tightened" until the spurious negative

values appearing between isentropic levels disappeared. This technique is illustrated in Fig. 2. Fig. 2a shows how a spline fit will naturally produce a negative value between points 2 and 3 when points 1 and 4 have large values and points 2 and 3, small values. A linear fit will remove this problem (Fig. 2b), but a more refined method can be used. The spline under tension can be adjusted so that the curve just reaches zero between points 2 and 3 (Fig. 2c). This is the desired result, since $|\nabla\theta|$ should have minima very close to, but not less than, zero.

Finally, the computer produces analyses of the various fields on microfilm. Figs. 3 through 22 show fields of θ , z , $dp/d\theta$, $|\vec{u}_{\text{bal}}|$, and $|\nabla\theta|$ for the case of 27 September 1970 at 00Z. The long tick marks around the edge show the NMC grid, the short marks, the interpolated grid.

The presence of incorrect soundings and superadiabatic layers caused many problems. The bad soundings had to be identified and weeded out. Nothing could be done about the superadiabats, but fortunately they occurred only around the edges of the analyses, most likely due to a bad first-guess field in the data-sparse regions. The spurious results they produced were not in the area of interest and could therefore be ignored. Usable analyses were obtained in fourteen of the cases:

10 October 1969, 00Z

22 October 1969, 00Z

11 January 1970, 00Z

14 January 1970, 00Z

16 January 1970, 00Z

26 January 1970, 00Z
12 March 1970, 00Z
5 September 1970, 00Z
6 September 1970, 00Z
7 September 1970, 00Z
27 September 1970, 00Z
16 December 1970, 00Z
16 December 1970, 12Z
17 December 1970, 00Z.

The aircraft observations for the 14 cases were each assigned to one of the four pressure levels, on a purely standard atmosphere basis, as follows:

24,000 to 28,000 ft - 350 mb
29,000 to 32,000 ft - 300 mb
33,000 to 36,000 ft - 250 mb
37,000 to 41,000 ft - 200 mb.

Reports from below 24,000 ft were discarded; there were none above 41,000 ft. Many of the reports were unusable for other reasons, such as the lack of a location report, or a simple "No report" for the intensity of turbulence. A total of 611 reports were collected from those which were made at radiosonde observation time or one hour either way of it.

The values of $dp/d\theta$ and $|\nabla\theta|$ for each observation were read off the appropriate charts and a geostrophic Richardson number

calculated. With the use of the hydrostatic relationship

$$\frac{\partial p}{\partial z} = -\rho g,$$

the thermal wind relationship

$$\frac{\partial |\vec{v}_g|}{\partial p} = \frac{R}{f_p} |\nabla T|,$$

and the ideal gas law

$$p\alpha = RT,$$

the formula for the Richardson number can be put in a usable form:

$$\begin{aligned} Ri &= \frac{g}{\theta} \frac{\partial \theta / \partial z}{|\partial \vec{v} / \partial z|^2} \\ &= -\frac{\alpha}{\theta} \frac{d\theta / dp}{|\partial \vec{v} / dp|^2} \\ &= -\frac{\alpha}{\theta} \frac{f^2 p^2}{R^2} \frac{d\theta / dp}{|\nabla T|^2} \\ &= -\frac{\alpha}{\theta} \frac{f^2 p^2}{R^2} \left(\frac{p_0}{p}\right)^{2\kappa} \frac{d\theta / dp}{|\nabla \theta|^2} \\ &= -\frac{f^2 p}{R} \left(\frac{p_0}{p}\right)^\kappa \frac{d\theta / dp}{|\nabla \theta|^2}. \end{aligned}$$

III. RESULTS

The analyses obtained through this procedure are illustrated in Figs. 3 through 22. These analyses show an area where clear-air turbulence would surely be expected. A well-marked upper-tropospheric front appears in conjunction with a broad trough in the height pattern. The region of strong horizontal temperature gradient coincides with a highly stable region (shown by low values of $dp/d\theta$ on the stability analyses), indicating the close packing of the θ -surfaces. The maximum wind speeds also lie along the front axis, as we would expect. A comparison of these analyses with the NMC analyses for twelve hours earlier and later (the analyses for the time of this case are missing from the M.I.T. collection) indicate that some improvement has been achieved.

The calculated Richardson numbers ranged in value from about 1 to over 1000, with a median of 25. In order to investigate the degree to which they are related to occurrences of clear-air turbulence, the chi-square test was used. The reports were ranked by Richardson number and divided into four equally-sized groups. The null hypothesis was that there is no relationship between Richardson number and clear-air turbulence, and, thus, each group should have the same percentage of reports with turbulence as does the sample as a whole. Chi-square was then evaluated from the difference between this expected number and the actual number of reports with turbulence in each group. In addition, the sample was divided into groups for a closer examination along the following lines:

whether the aircraft was located on a cyclonically or an anticyclonically curved contour, whether or not the aircraft was over mountainous terrain (taken to be west of 100°W longitude), and whether the case as a whole had a maximum jet-stream speed of more or less than 60 m sec^{-1} (chosen so that the two groups would have seven cases each). The results for these various groups are summarized in Table 1. The last column gives the probability, according to the chi-square test, of this marked a relation occurring by chance, were there no actual correlation.

The chi-square test can tell us if there is skill involved in making a forecast, but not very much about how much skill. For this reason, Table 1 also includes the medians of the reports with turbulence and of those without turbulence, the idea being that the greater the difference between the medians, the better the forecaster the Richardson number will be.

Several things of a general nature are immediately apparent in the table. First, the percentage of reports with turbulence is always approximately 40. This is clear evidence that the sample is very biased, since a truly random sample would probably not have one tenth this many. Second, the value of chi-square is tied to the number of reports in the group. The relatively high level of significance shown by the total collection of reports is no doubt due to the fact that it includes the most cases. And third, the mean is everywhere higher than the median. This is merely an indication of the highly skewed nature of the distribution, which comes as no surprise.

A closer inspection reveals some not-so-expected results.

The average Richardson number is smaller for the cyclonic cases than for the anticyclonic ones. This is evidently a weakness of the geostrophic approach. We would expect the anticyclonic curvature to cause generally larger wind speeds and consequently larger shears, as previously noted. However, both the chi-square and the difference of medians indicate that clear-air turbulence would be better forecast in the instances where the curvature is anticyclonic.

The chi-square test gives a much weaker correlation for the mountain reports than for the non-mountain ones, but this is probably at least partly due to the larger number of non-mountain reports. However, we would anticipate a weaker correlation in the mountains because of the presence of mountain-wave induced turbulence which could hardly be handled very well with this type of approach. It is interesting to note that the difference between medians is much larger for the mountain reports, the reason for which is not immediately apparent.

The two groups determined by the maximum jet-stream speed also exhibit some interesting features. The groups are very nearly the same size, so there must be some other reason for the better correlation in the weaker jet-stream group, shown by both the chi-square and the difference of medians. It is not surprising that the cases with the jet maximum over 60 m sec^{-1} have much smaller average Richardson numbers, but this does not apparently help the correlation.

IV. CONCLUSIONS

The results of this investigation are, it would seem, sufficient to demonstrate the value of this type of approach in predicting regions of possible clear-air turbulence. The results themselves, however, are perhaps not as important as the indications they give as to how this technique might be improved, in both the procedure used in gathering the aircraft reports as well as in the method of calculating the Richardson numbers.

The collection of reports that was used is probably biased in many ways. The most obvious of these, as mentioned before, is the unrepresentatively large proportion of reports with turbulence. Granted that the way in which the cases were chosen has no doubt worsened this aspect, the entire collection of 68,000 reports is unquestionably also biased in this respect. It was most likely brought about by the voluntary nature of the pilot participation in the program.* It is only natural that a pilot is much more likely to make a report if there is turbulence than if there is not. Another possible bias is the distribution of aircraft in the air as a function of time of day, with maxima in mid-morning and late evening. The correlation, if any, between occurrences of clear-air turbulence and time of day is not at all clear, but could be an effect. The fact that American's flights are largely restricted to a northeast-southwest strip through the country may

* Personal communication with P. E. Kraght of American Airlines.

limit the portions of the jet stream through which they fly, and thus affect the sample. Although not a bias as such, having locations only to the nearest degree and times only to the nearest hour certainly diminishes the usefulness of such reports. A horizontal temperature gradient can obviously go from very strong to very weak in less than the distance covered in a half-hour's flying time at modern jet speeds.

On the basis of these observations, some recommendations to the airlines for future programs of this sort might be in order. Such recommendations would include

- 1) Industry-wide participation to obtain better coverage of the entire country,
- 2) Locations given to the nearest tenth of a degree and times to the nearest minute, and
- 3) Participation by all the pilots in the air.

It is too much to hope for all of this, but any of it would be a step in the right direction.

The method by which the Richardson numbers were calculated could also be considerably improved upon. The most obvious way would be to try to locate the aircraft more exactly in three-space rather than assigning it to some arbitrary pressure level. For example, the radiosonde observations nearest the aircraft could be used to determine its pressure level and the values of stability and shear could be evaluated for that exact point. It

would also be a good idea to reexamine the possibility of using real wind data, or at least a gradient rather than a geostrophic or balanced wind approach. A proper filtering procedure, such as the one used by Bosart, should be able to make this feasible. A further refinement, though perhaps a very difficult one, would be to allow for translation of the synoptic features in the case of reports which do not fall exactly on observation times.

Most of these improvements would be appropriate for future studies of this type. However, on a real-time forecasting basis, they might not be usable, at least not at present, because of computer time restrictions.

In conclusion, it must be remembered that outstandingly good results were not expected due to the fine-scale nature of clear-air turbulence and the coarseness of the radiosonde network. The crudeness of the analysis procedure and the lack of precision in the aircraft reports makes it quite possible that some of the Richardson numbers were calculated for points quite far from where the airplane actually was, not to mention that it might be for the wrong time, too. Bearing all this in mind, the results are encouraging enough to demonstrate the usefulness of fine-scale isentropic analysis and the worthwhileness of pursuing this kind of research further.

	(1)	(2)	(3)	(4)	(5)	(6)	(7)
Total	611	40.8	60	25	17	28	<0.1%
Mountain	174	44.2	84	35	25	46	15%
Non-mountain	437	39.3	50	20	17	24	3%
Cyclonic	344	38.8	54	20	18	23	18%
Anticyclonic	267	43.5	67	27	19	33	1.5%
Jet max \geq 60 m sec⁻¹	318	39.6	43	16	14	17	24%
Jet max < 60 m sec⁻¹	293	41.9	77	41	38	43	9%

- (1) Number of reports
- (2) Percentage of reports with turbulence
- (3) Mean Ri
- (4) Median Ri
- (5) Median Ri of reports with turbulence
- (6) Median Ri of reports without turbulence
- (7) Probability of relation occurring by chance

Table 1

NMC OCTAGONAL GRID

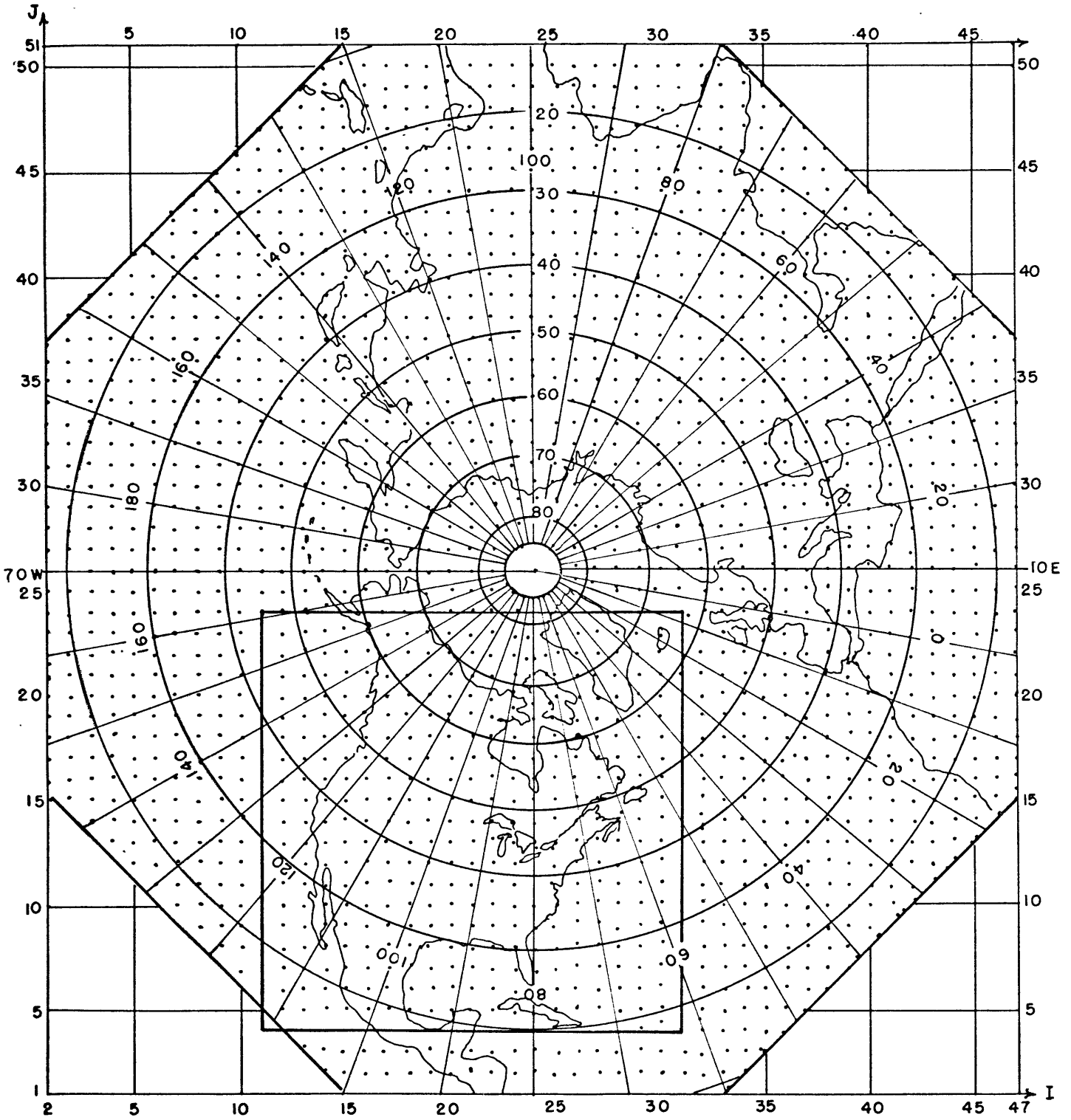


Fig. 1

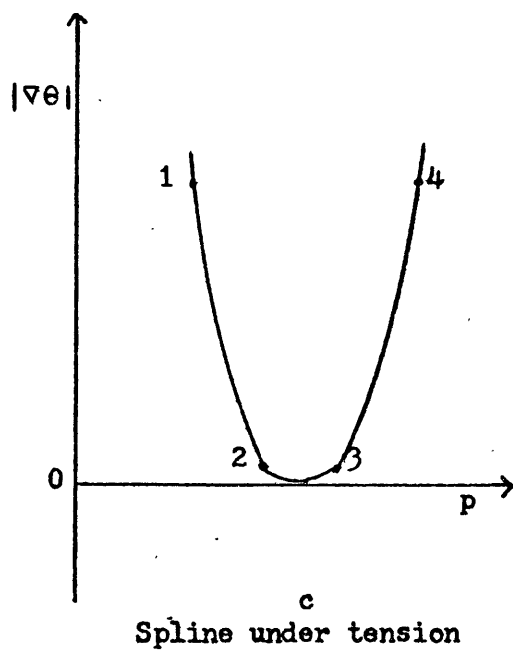
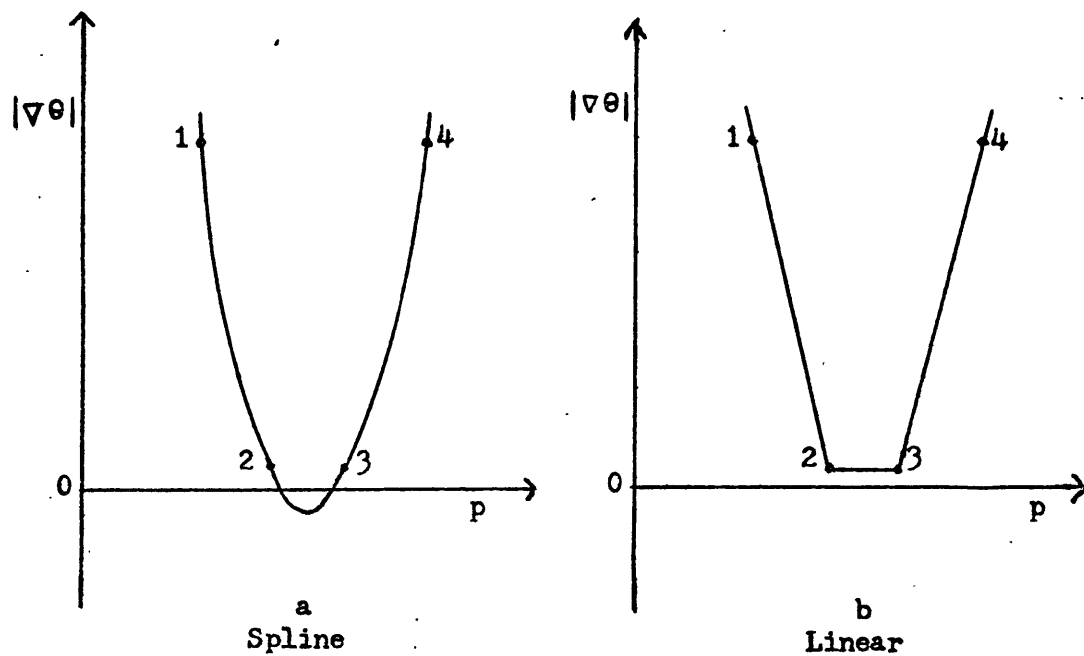
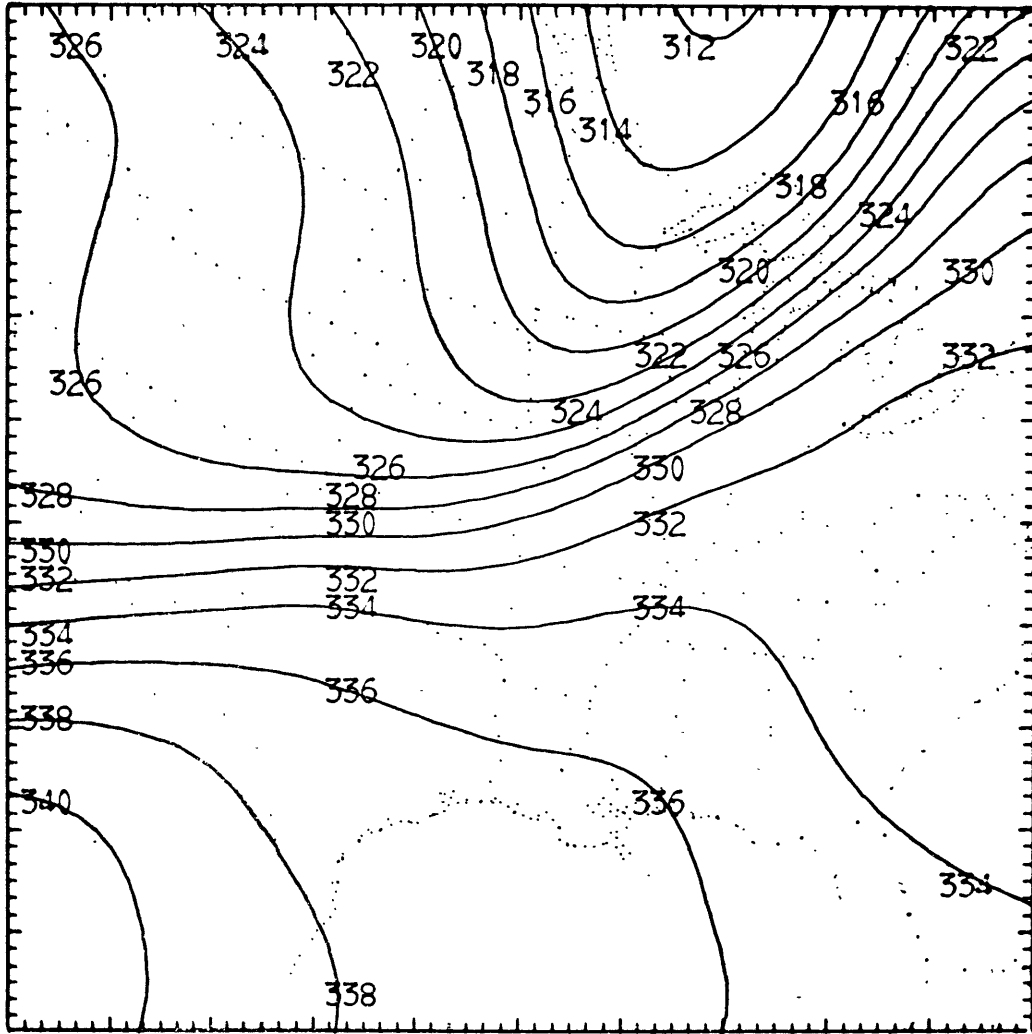


Fig. 2



70092700 POTENTIAL TEMPERATURE 350 MB

CONTOUR FROM 3.100E+02 TO 3.400E+02 CONTOUR INTERVAL OF 2.000E+00 SCALED BY 1E+00 PT(5,5) = 3.411E+02

Fig. 3
Contour interval: 2°K

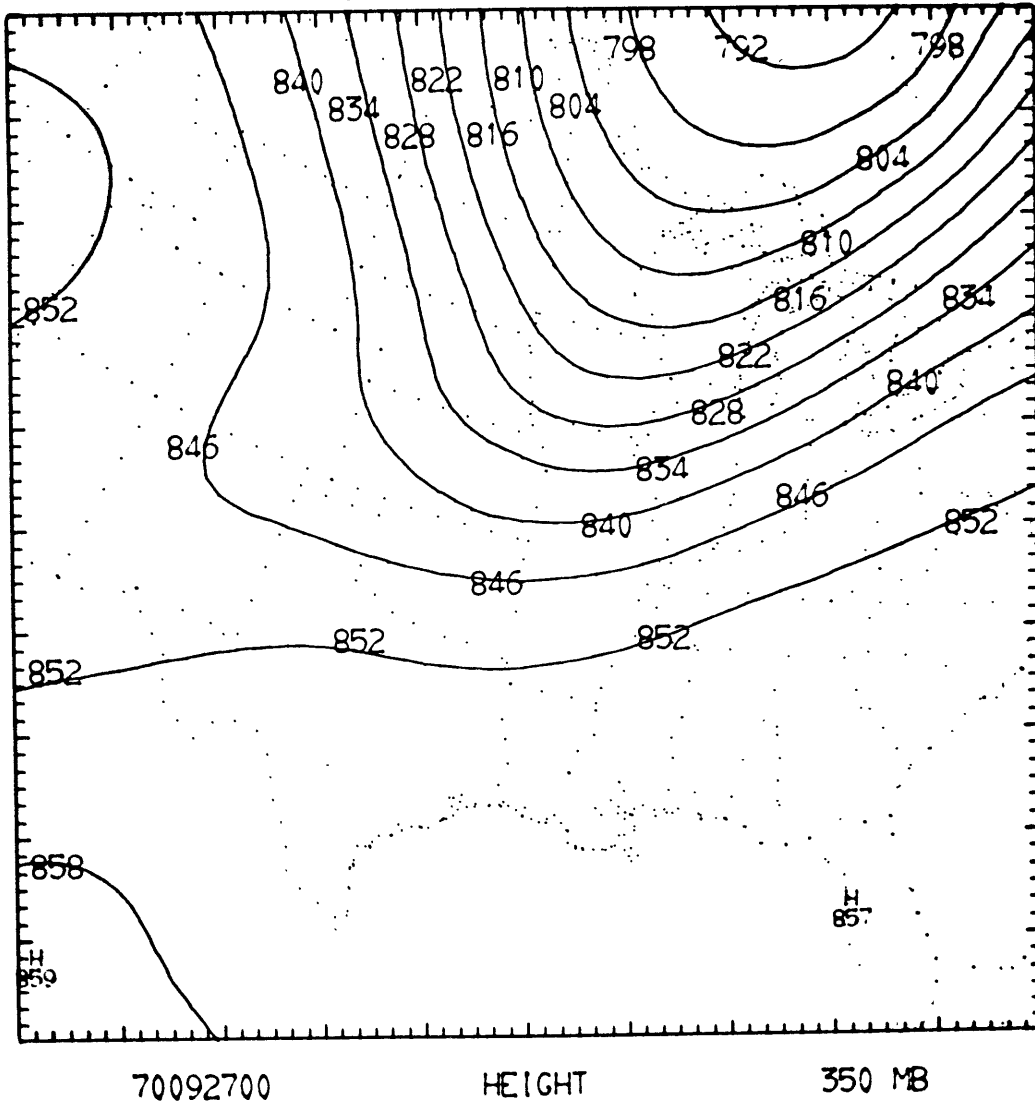
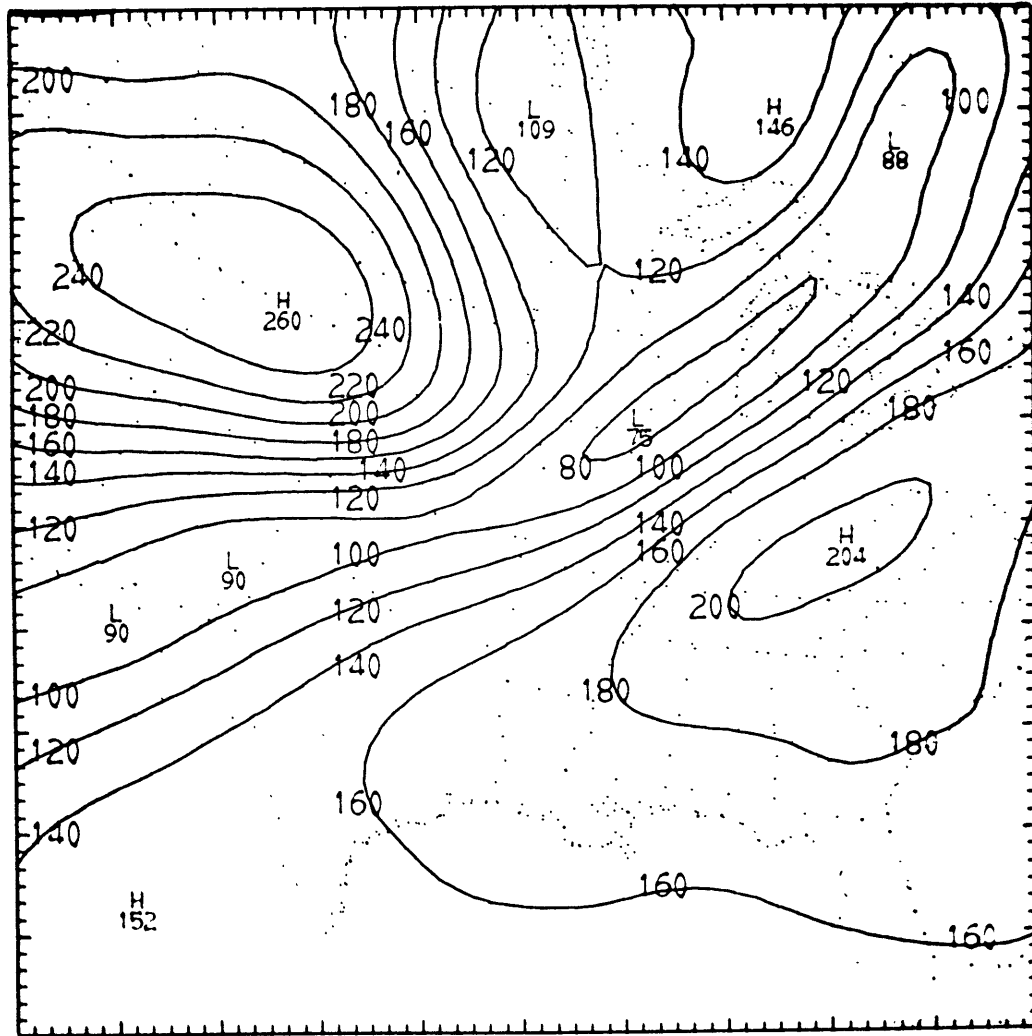


Fig. 4
Contour interval: 60 m



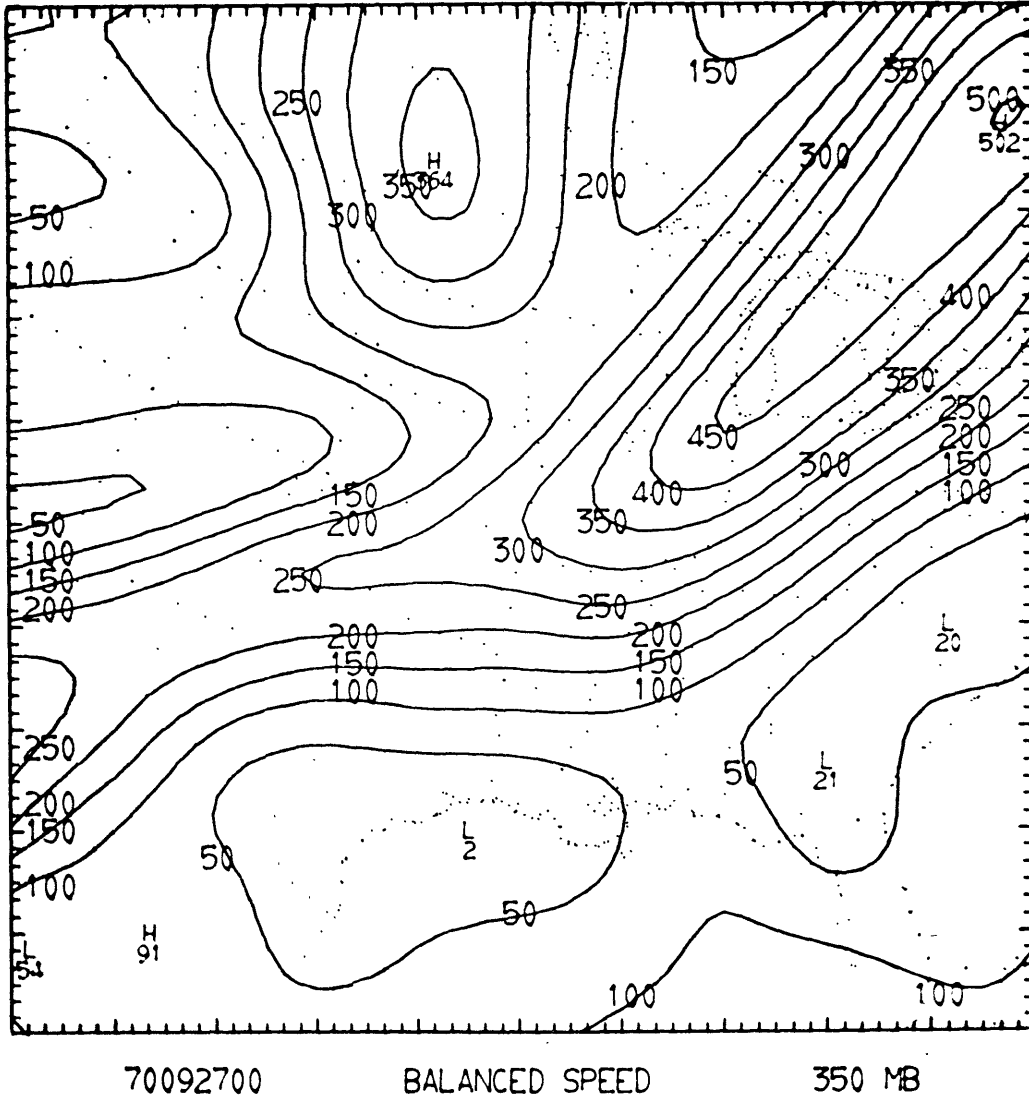
70092700

STABILITY

350 MB

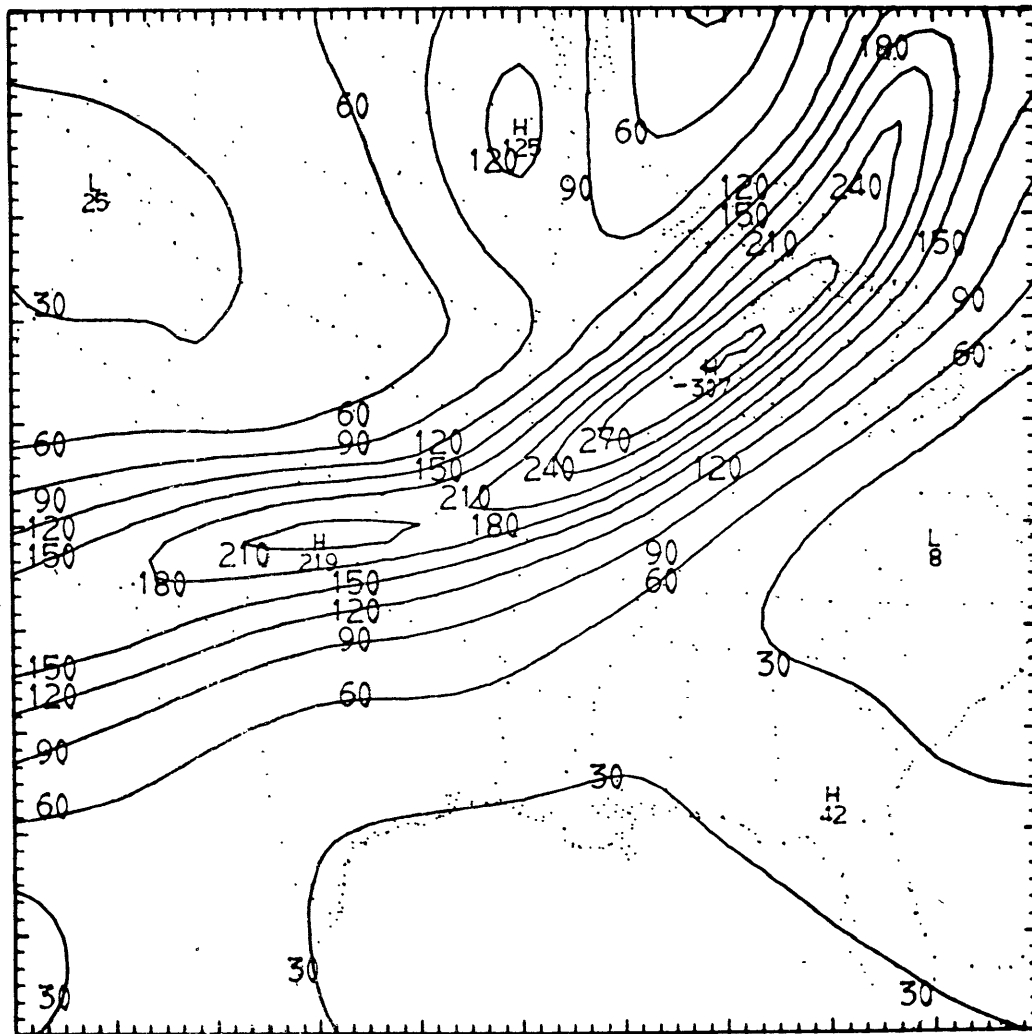
CONTOUR FROM 6.000E-03 TO 2.400E-02 CONTOUR INTERVAL OF 2.000E-03 SCALED BY 1E+04 PT(3,3) = 1.469E-02

Fig. 5
Contour interval: 2 mb °K⁻¹



CONTOUR FROM 0.0 TO 5.000E+01 CONTOUR INTERVAL OF 5.000E+00 SCALED BY 1E+01 PT(9,91) = 7.371E+00

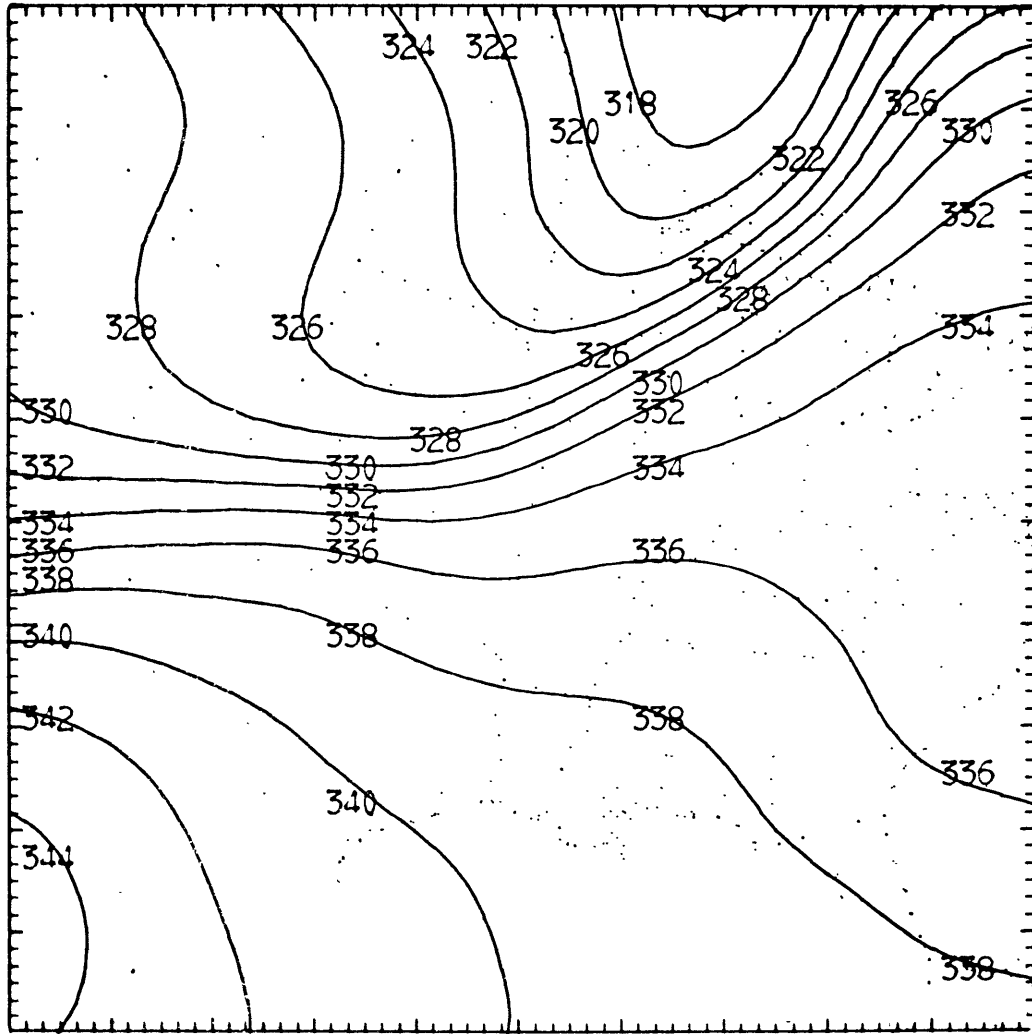
Fig. 6
Contour interval: 5 m sec⁻¹



70092700 GRADIENT OF POTENTIAL TEMP 350 MB

CONTOUR FROM 0.0 TO 5.000E-07 CONTOUR INTERVAL OF 3.000E-08 SCALED BY 1E+09 PT(3.31) 2.794E-08

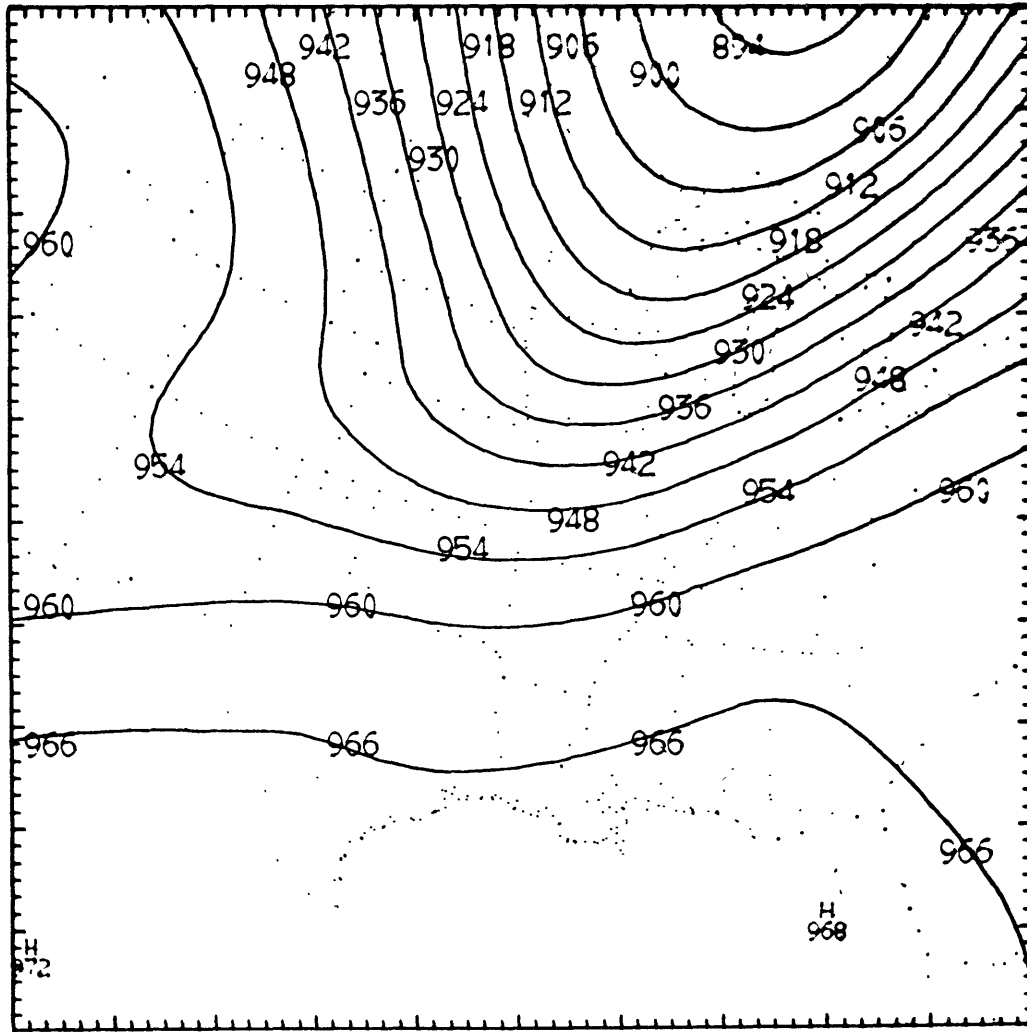
Fig. 7
 Contour interval: $.3^{\circ}\text{K} (100 \text{ km})^{-1}$



70092700 POTENTIAL TEMPERATURE 300 MB

CONTOUR FROM 3.140E+02 TO 3.440E+02 CONTOUR INTERVAL OF 2.000E+00 SCALED BY 1E+00 PT(3,3) = 3.443E+02

Fig. 8
Contour interval: 2°K



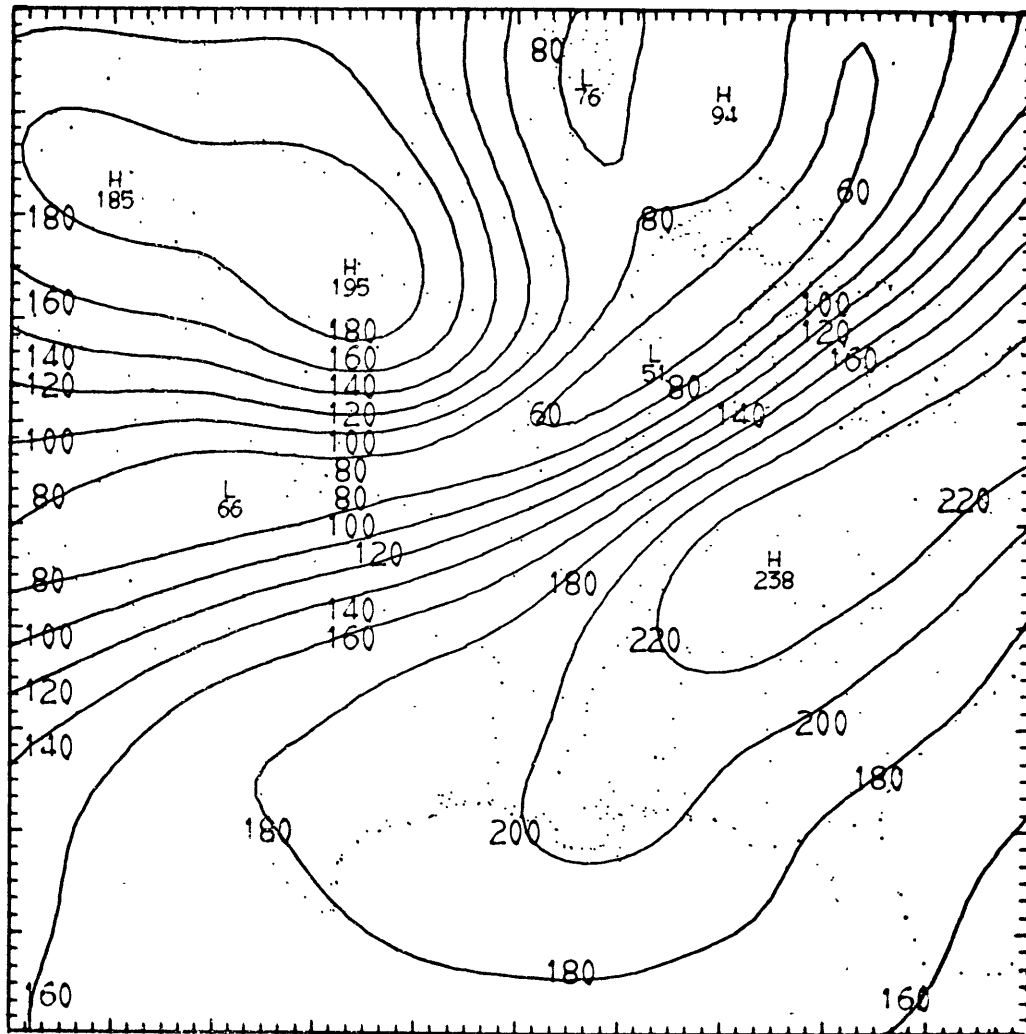
70092700

HEIGHT

300 MB

CONTOUR FROM 8.800E+01 TO 9.660E+01 CONTOUR INTERVAL OF 6.000E-01 SCALED BY 1E+01 PT(3,31) = 9.719E+01

Fig. 9
Contour interval: 60 m



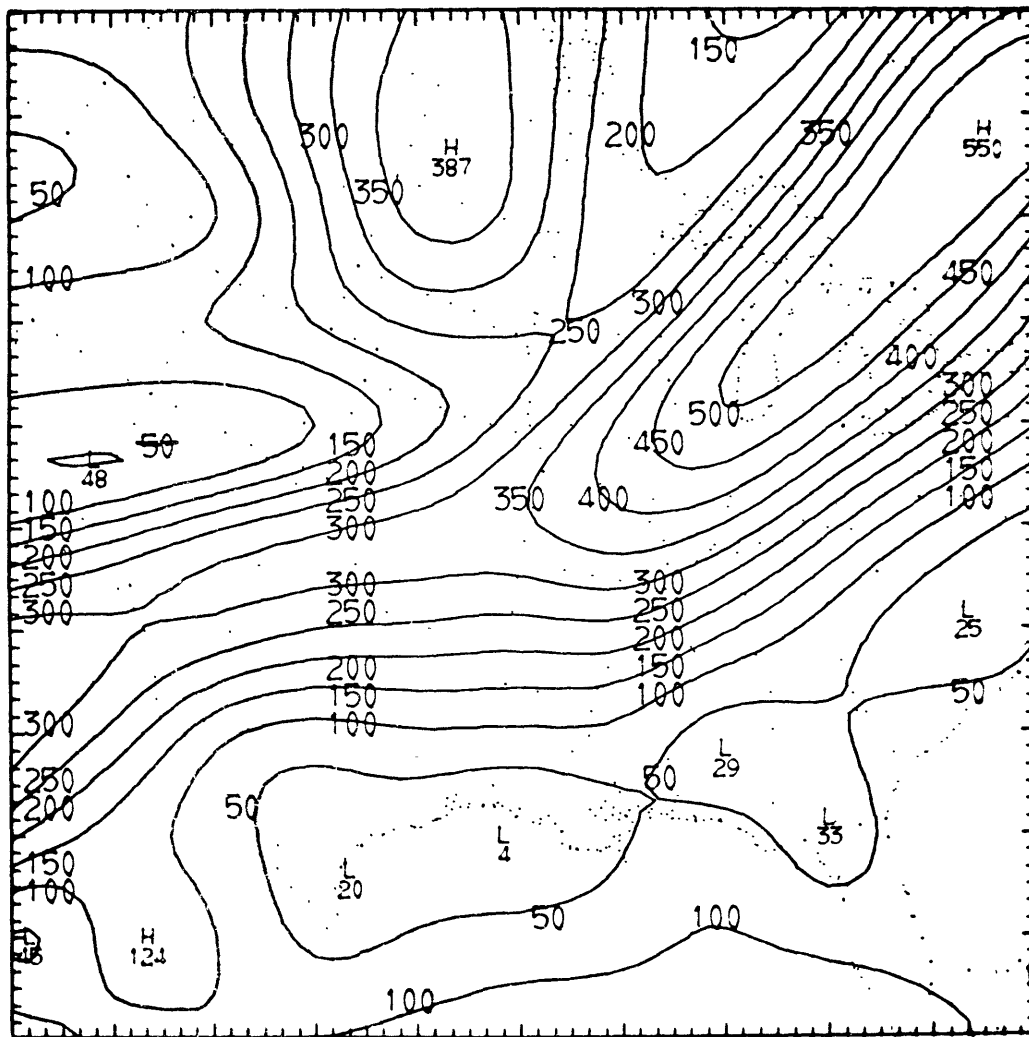
70092700

STABILITY

300 MB

CONTOUR FROM 4.000E-03 TO 2.200E-02 CONTOUR INTERVAL OF 2.000E-03 SCALED BY 1E+04 PT(3,3) = 1.639E-02

Fig. 10
Contour interval: 2 mb °K⁻¹



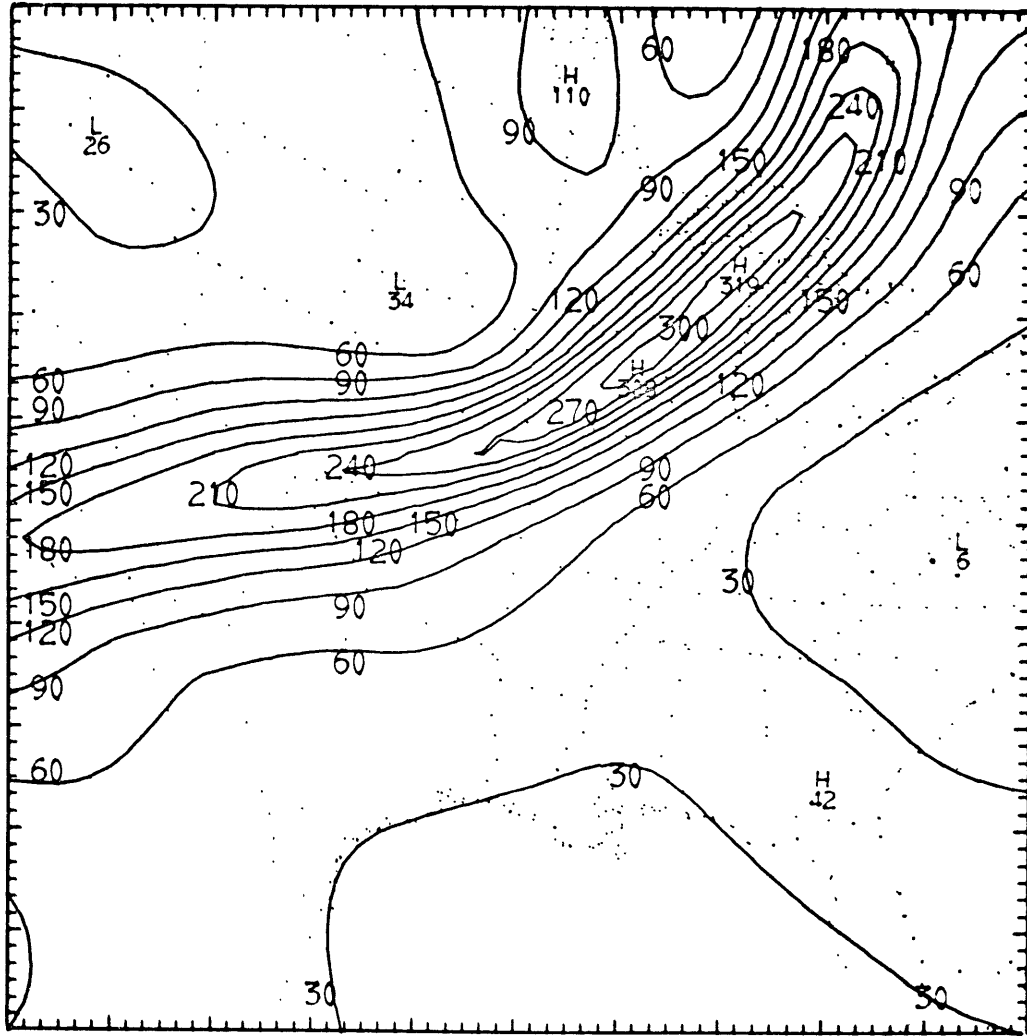
70092700

BALANCED SPEED

300 MB

CONTOUR FROM 0.0 TO 5.000E+01 CONTOUR INTERVAL OF 5.000E+00 SCALED BY 1E+01 PT(3,3) 0.902E+00

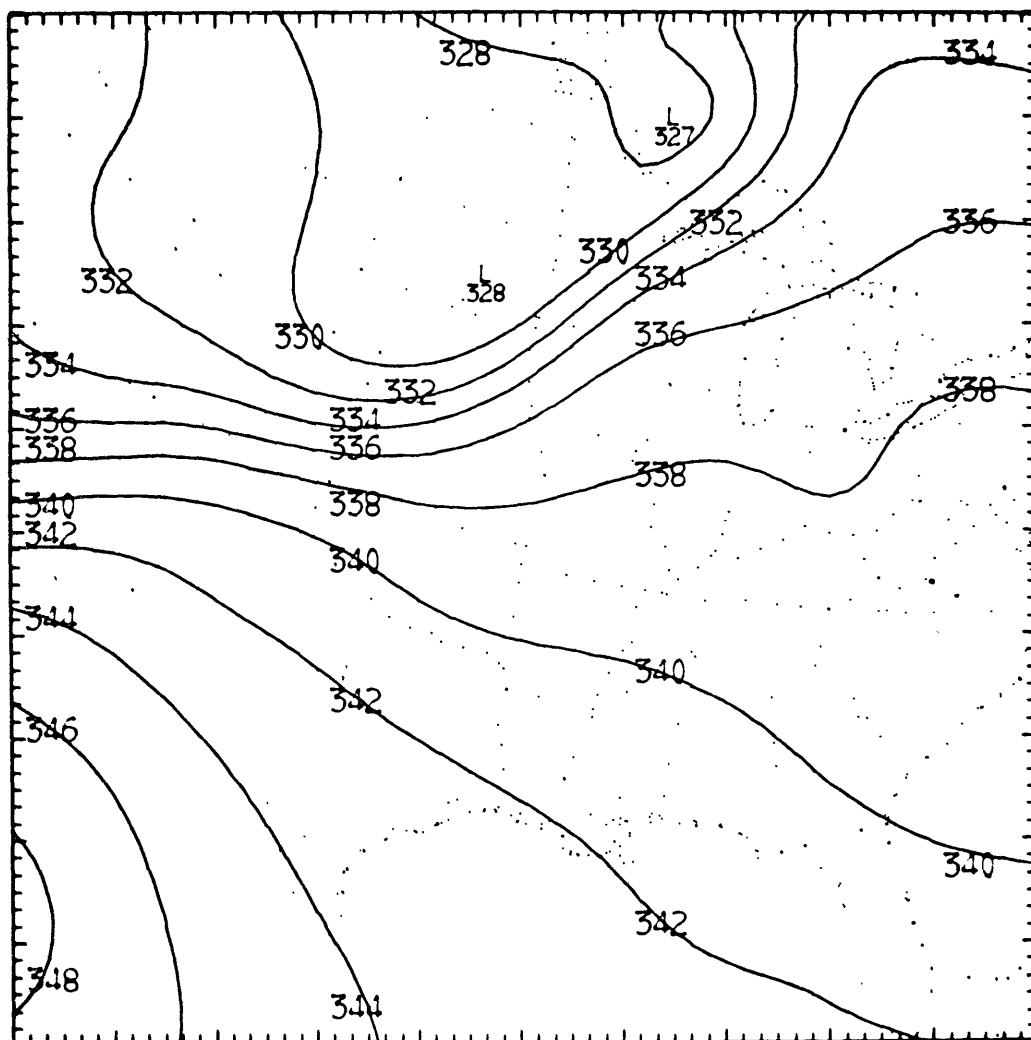
Fig. 11
Contour interval: 5 m sec⁻¹



70092700 GRADIENT OF POTENTIAL TEMP 300 MB

CONTOUR FROM 0.0 TO 3.000E-07 CONTOUR INTERVAL OF 3.000E-08 SCALED BY 1E+09 PT(3,31) = 3.219E-08

Fig. 12
 Contour interval: $.3^{\circ}\text{K} (100 \text{ km})^{-1}$



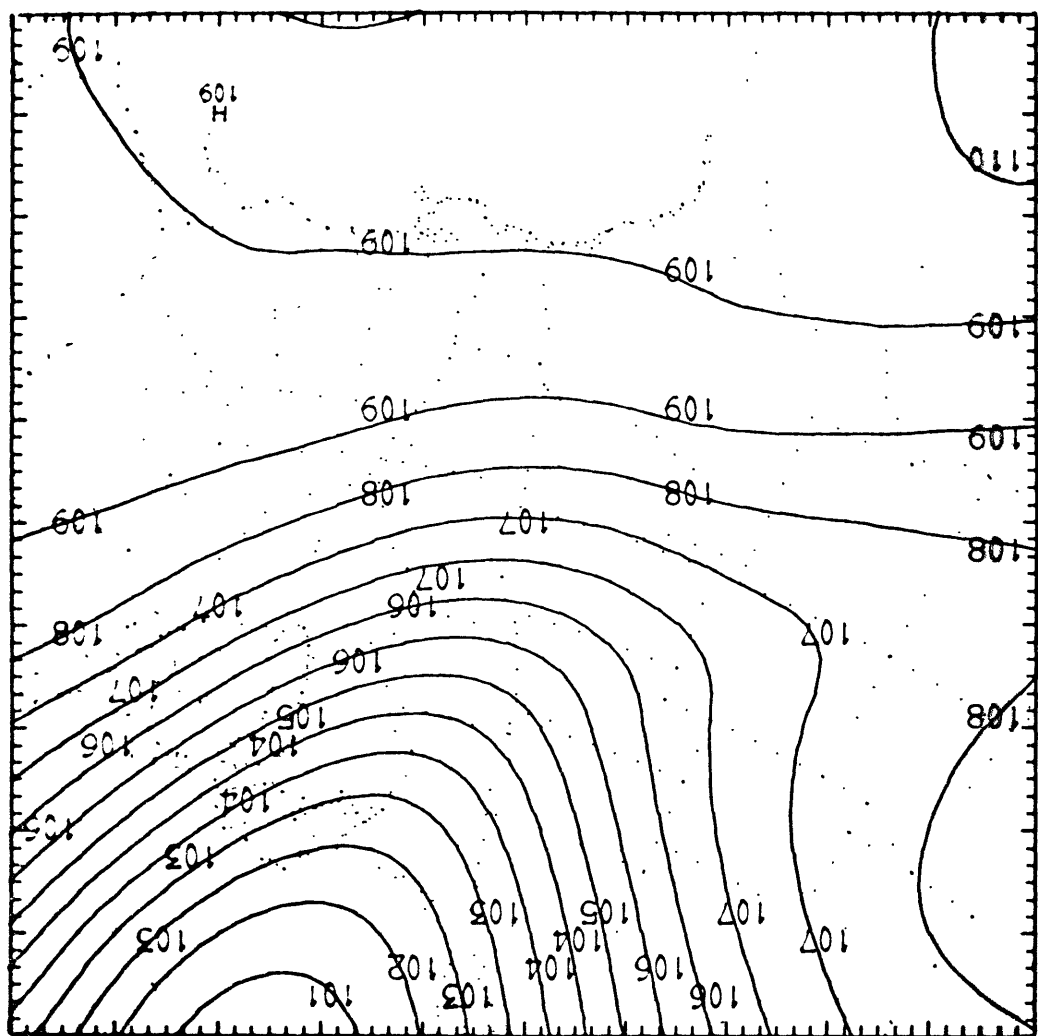
70092700 POTENTIAL TEMPERATURE 250 MB

CONTOUR FROM 3.260E+02 TO 3.480E+02 CONTOUR INTERVAL OF 2.000E+00 SCALED BY 1E+00 PT(3,31)= 3.477E+02

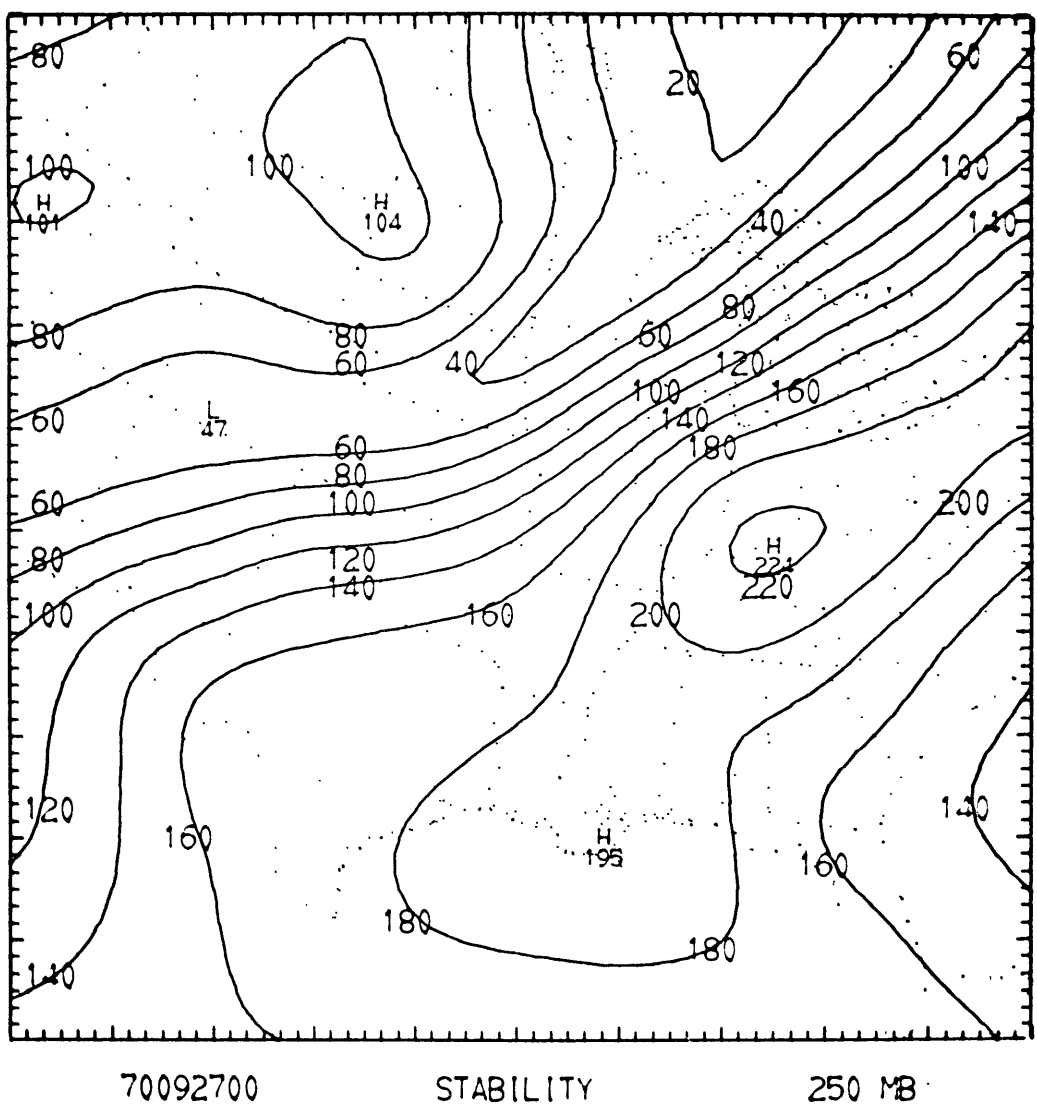
Fig. 13
Contour interval: 2°K

Fig. 14
Contour Interval: 60 m

70092700
HEIGHT
250 MB

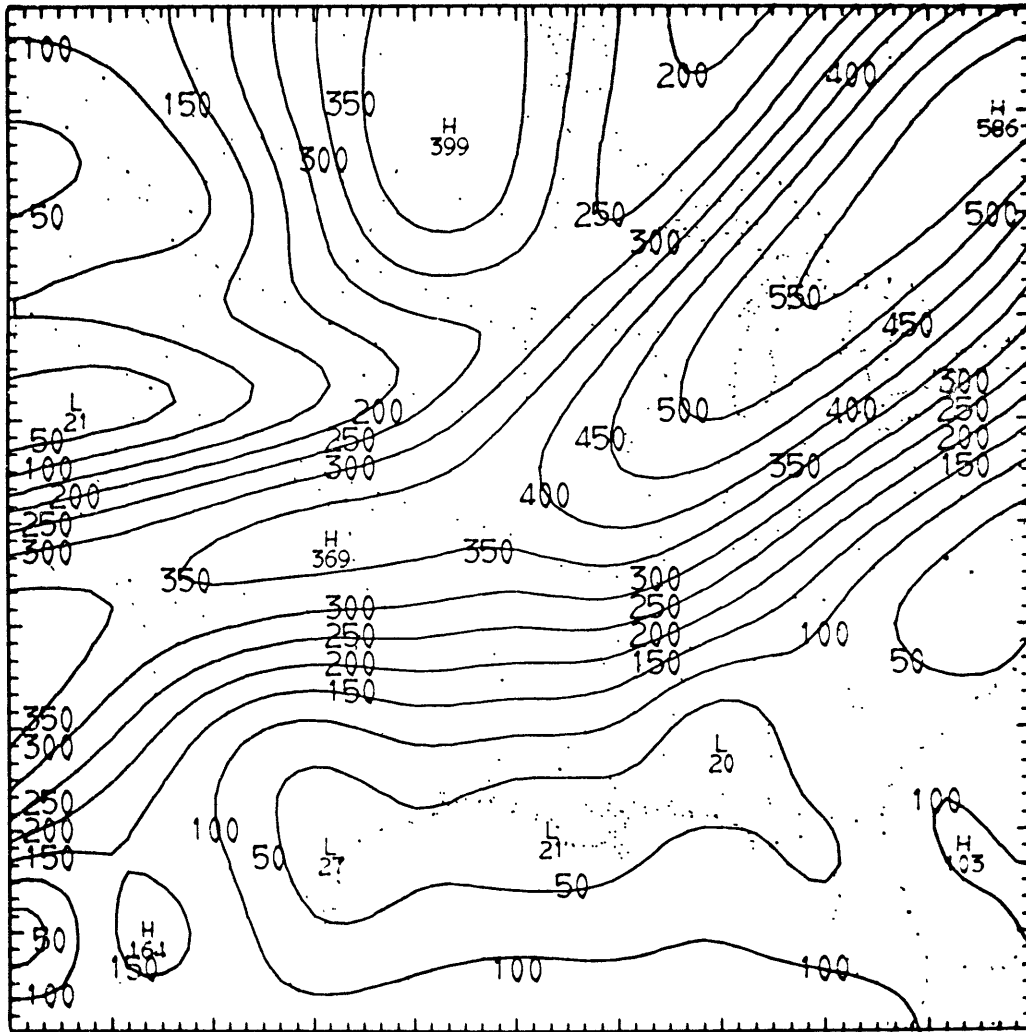


CONTOUR FROM 1.000E+02 TO 1.090E+02 CONTOUR INTERVAL OF 6.000E-01 SCALED BY 1E+00 P1715.31 - 1.090E+02



CONTOUR FROM 0.0 TO 2.200E-02 CONTOUR INTERVAL OF 2.000E-03 SCALED BY 1E+04 PT(15,3) = 1.450E-02

Fig. 15
Contour interval: 2 mb °K⁻¹



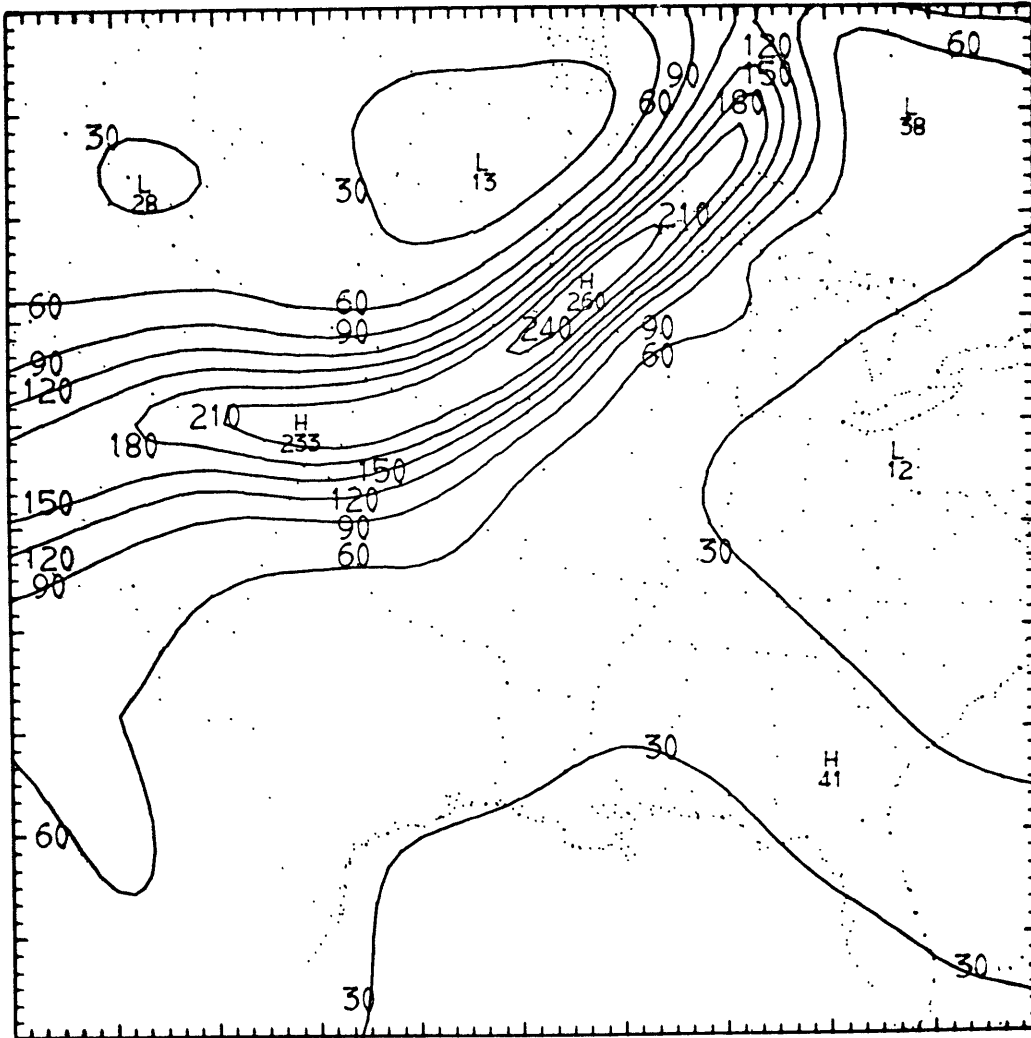
70092700

BALANCED SPEED

250 MB

CONTOUR FROM 0.0 TO 5.500E+01 CONTOUR INTERVAL OF 5.000E+00 SCALED BY 1E+01 PT(3,3) = 1.045E+01

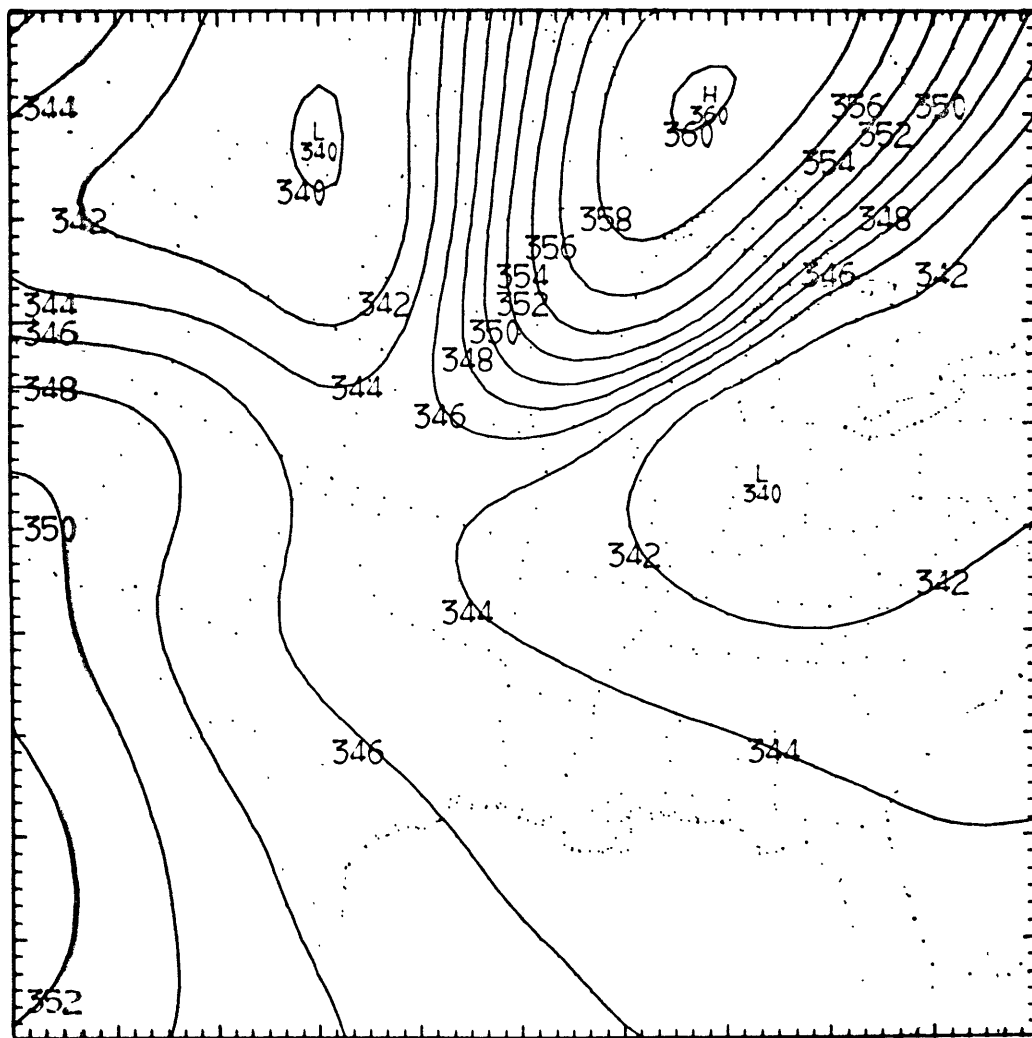
Fig. 16
Contour interval: 5 m sec⁻¹



70092700 GRADIENT OF POTENTIAL TEMP 250 MB

CONTOUR FROM 0.0 TO 2.400E-07 CONTOUR INTERVAL OF 3.000E-08 SCALED BY 1E+09 PT(3,3) = 4.109E-08

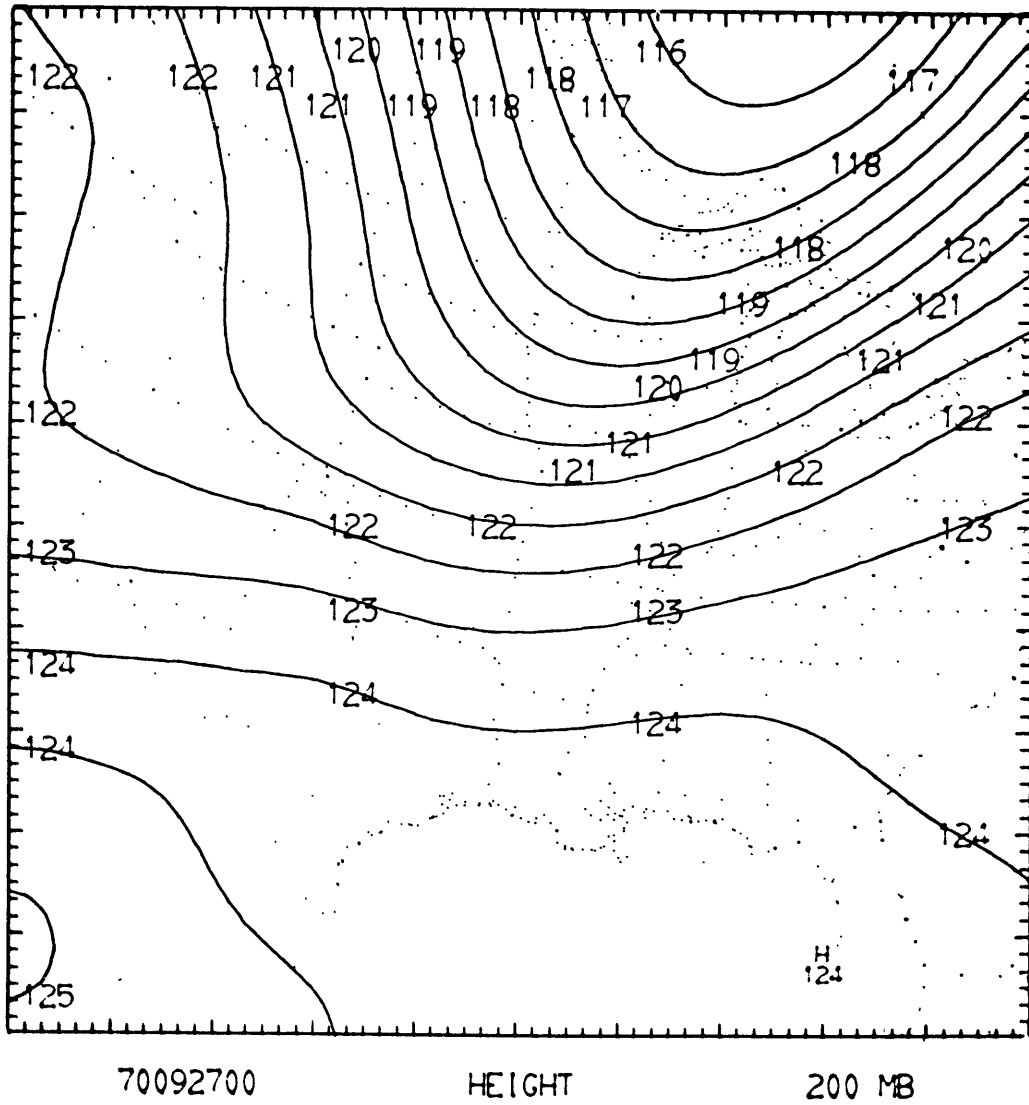
Fig. 17
Contour interval: $.3^{\circ}\text{K} (100 \text{ km})^{-1}$



70092700 POTENTIAL TEMPERATURE 200 MB

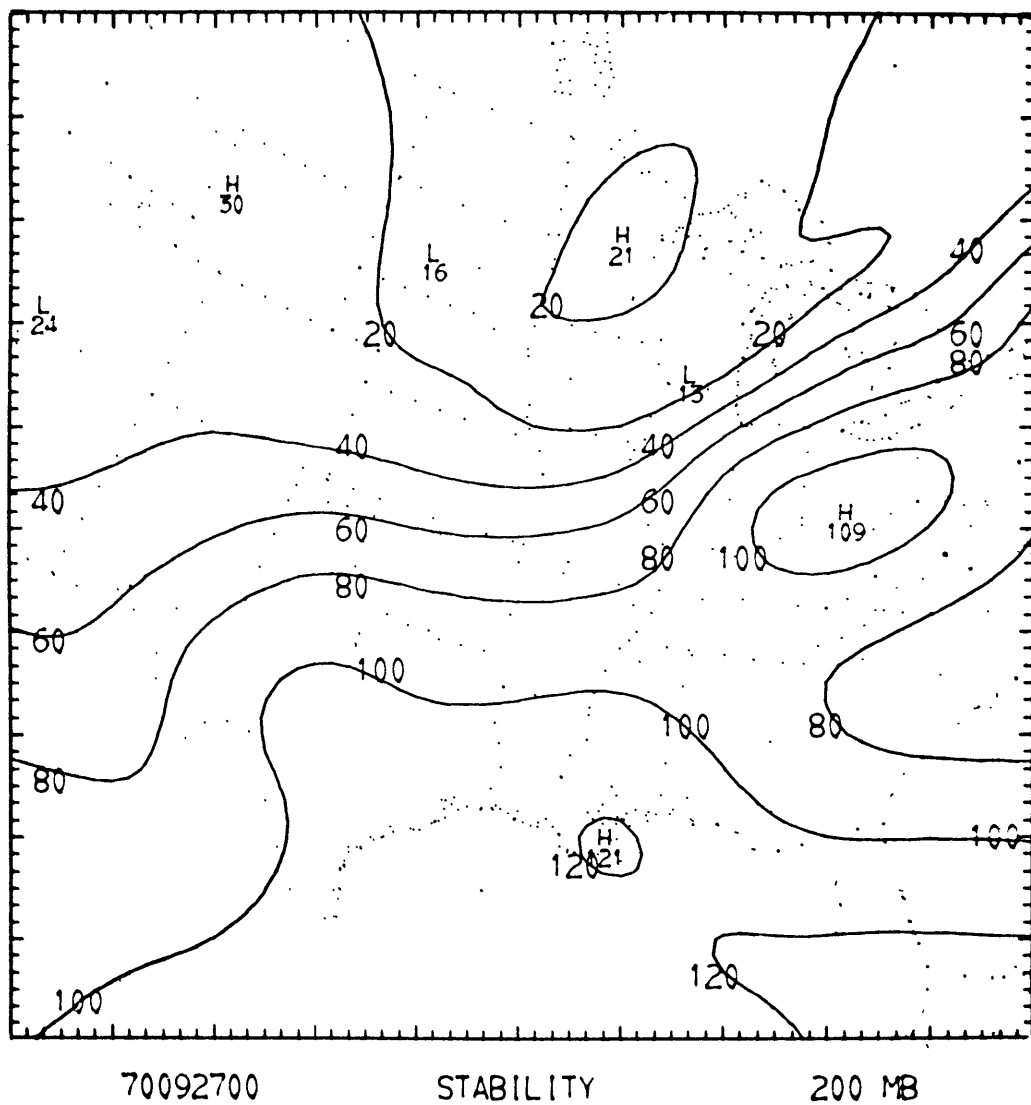
CONTOUR FROM 3.380E+02 TO 3.600E+02 CONTOUR INTERVAL OF 2.000E+00 SCALED BY 1E+00 PT(3,3)= 3.519E+02

Fig. 18
Contour interval: 2°K



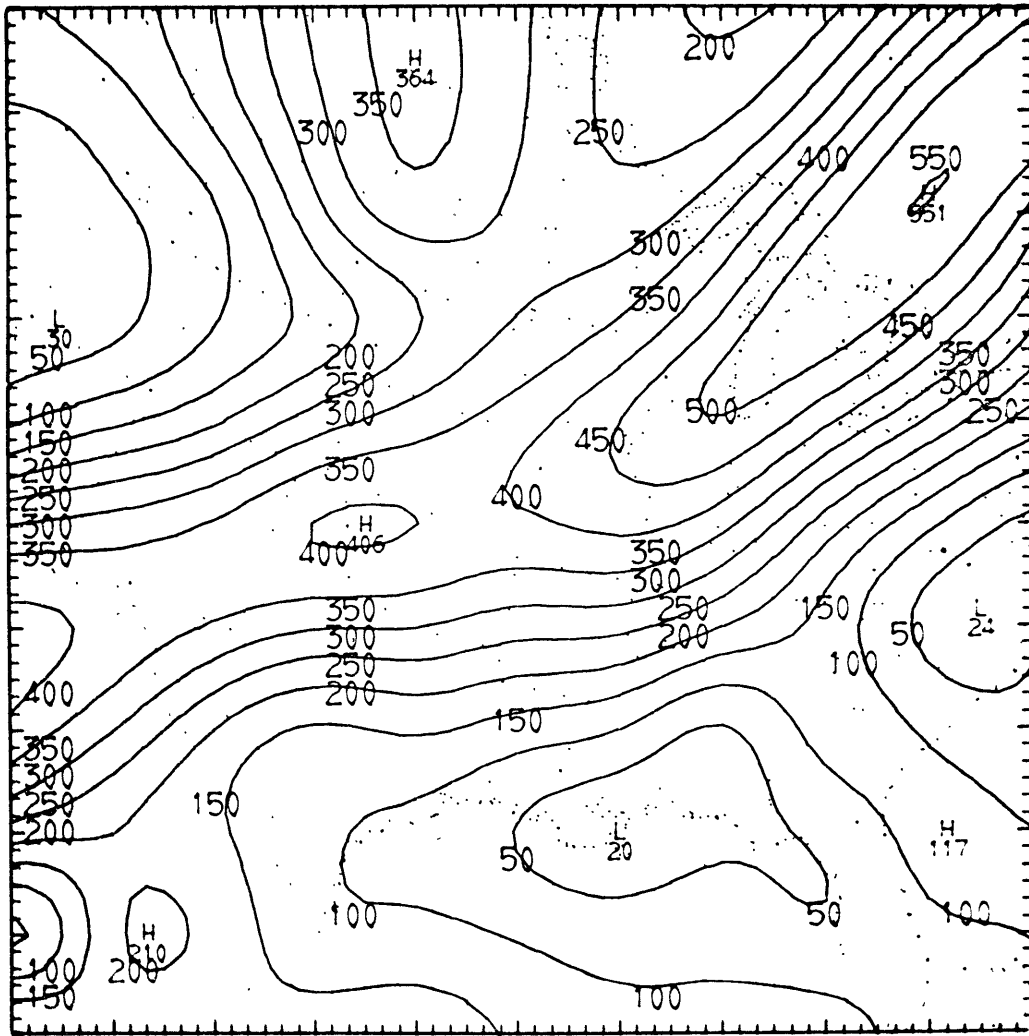
CONTOUR FROM 1.160E+02 TO 1.240E+02 CONTOUR INTERVAL OF 6.000E-01 SCALED BY 1E+00 PT(5,5) = 1.240E+02

Fig. 19
Contour interval: 60 m



CONTOUR FROM 0.0 TO 1.200E-02 CONTOUR INTERVAL OF 2.000E-03 SCALED BY 1E+04 PT(5,3) = 9.798E-03

Fig. 20
Contour interval: 2 mb °K⁻¹



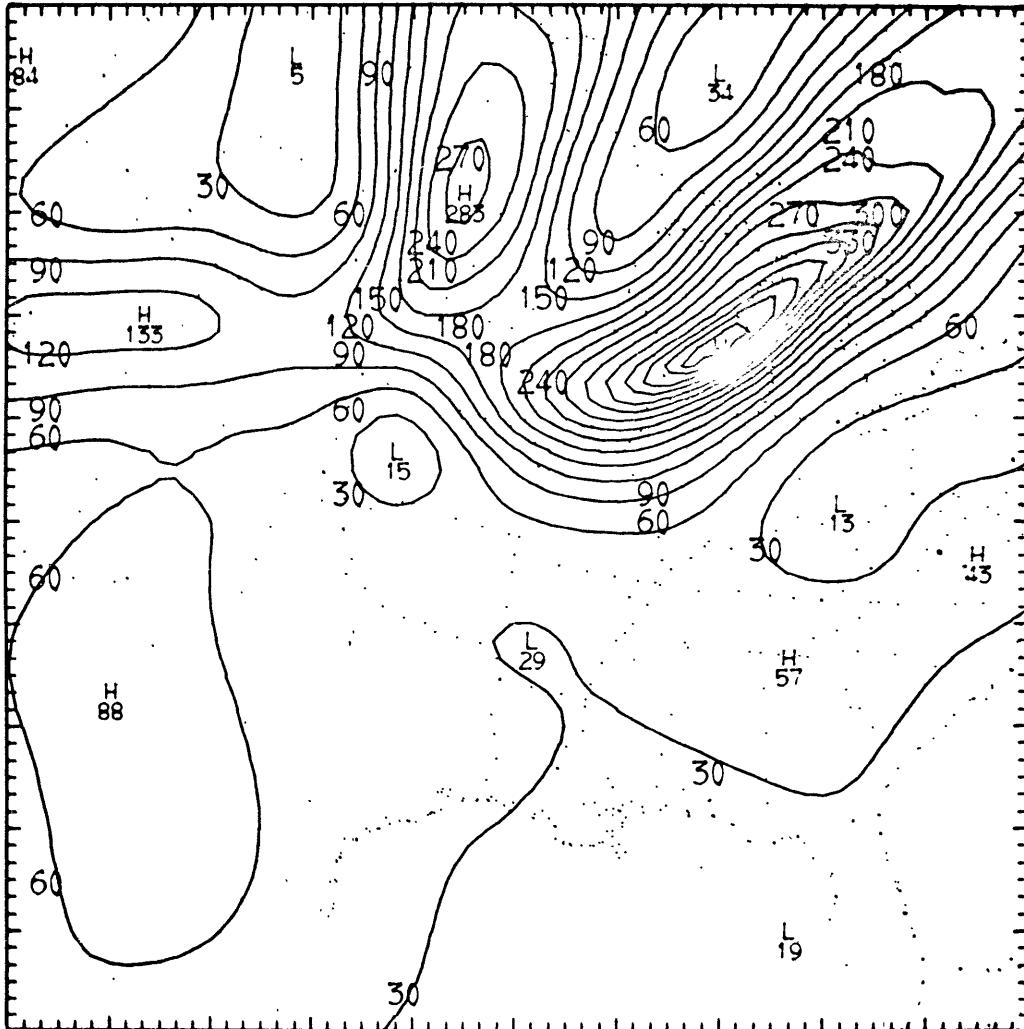
70092700

BALANCED SPEED

200 MB

CONTOUR FROM 0.0 TO 5.500E+01 CONTOUR INTERVAL OF 5.000E+00 SCALED BY 1E+01 PT(3,3) = 1.545E+01

Fig. 21
Contour interval: 5 m sec⁻¹



70092700 GRADIENT OF POTENTIAL TEMP 200 MB

CONTOUR FROM 0.0 TO 4.800E-07 CONTOUR INTERVAL OF 3.000E-08 SCALED BY 1E+09 PT(3,3) = 5.251E-08

Fig. 22
Contour interval: $.3^{\circ}\text{K} (100 \text{ km})^{-1}$

REFERENCES

- Bleck, R., and P. L. Haagenson, 1968: Objective analysis on isentropic surfaces. NCAR Technical Note No. 39, 27 pp.
- Bosart, L. F., 1969: Mid-tropospheric frontogenesis and potential vorticity behavior. Ph.D. thesis, M.I.T., 132 pp.
- Browning, K. A., 1971: Structure of the atmosphere in the vicinity of large-amplitude Kelvin-Helmholtz billows. Quart. J. Roy. Met. Soc. 97, 283-299.
- Danielsen, E. F., 1959: The laminar structure of the atmosphere and its relation to the concept of a tropopause. Arch. Met. Geoph. Biolk., Ser. A, Band II, 3 Heft, 294-332
- Eddy, A., 1967: Statistical objective analysis of scalar data fields. J. Appl. Met. 6, 597-609
- Lutz, M. P., 1972: Isentropic objective analysis applied to fine-scale analysis on isobaric surfaces. Summary reports-Fellowship in Scientific Computing, summer 1972. NCAR Technical Note Proc-80, 67-78.
- Montgomery, R. B., 1937: A suggested method for representing gradient flow in isentropic surfaces. Bull. Amer. Met. Soc. 18, 210-212.
- Nilson, E. N., 1970: Cubic splines on uniform meshes. Comm. ACM 13, 255-258.
- Panofsky, H. A., J. A. Dutton, K. H. Hemmerich, G. McCreary, and N. V. Loving, 1968: Case studies of the distribution of CAT in the troposphere and stratosphere. J. Appl. Met. 7, 384-389.
- Reed, R. J., 1969: A study of the relationship of clear air turbulence to the mesoscale structure of the jet stream region. Clear air turbulence and its detection, Plenum Press, New York, 288-306
- Reed, R. J., and K. R. Hardy, 1972: A case study of persistent, intense, clear air turbulence in an upper level frontal zone. J. Appl. Met. 11, 541-549.
- Richardson, L. F. 1920: The supply of energy from and to atmospheric eddies. Proc. Roy. Soc. A 97, 354-372.

- Schweikert, D. G., 1966: An interpolation curve using a spline under tension. *J. Mathematics and Physics* 45, 312-317.
- Seaman, N. L., 1972: The calculation of a semi-balanced stream function field from a given Montgomery stream function field. Summary reports--Fellowship in Scientific Computing, summer 1972, NCAR Technical Note Proc-80, 79-92.
- Taylor, G. I., 1931: Effect of variation in density on the stability of superposed streams of fluid. *Proc. Roy. Soc. A* 132, 499-523.
- Waco, D. E., 1972: Temperature gradients in stratospheric turbulence. *J. Appl. Met.* 11, 99-107.
- Walsh, J. L., H. J. Ahlberg, and E. N. Nilson, 1962: Best approximation properties of the spline fit. *J. Mathematics and Mechanics* 11, 225-234.